Journal of Histochemistry & Cytochemistry 59(2) 129–138

DOI: 10.1369/0022155410394857
http://jhc.sagepub.com
SAGE

Light Sheet Fluorescence Microscopy: A Review

Peter A. Santi

Department of Otolaryngology, University of Minnesota, Minneapolis

Summary

Light sheet fluorescence microscopy (LSFM) functions as a non-destructive microtome and microscope that uses a plane of light to optically section and view tissues with subcellular resolution. This method is well suited for imaging deep within transparent tissues or within whole organisms, and because tissues are exposed to only a thin plane of light, specimen photobleaching and phototoxicity are minimized compared to wide-field fluorescence, confocal, or multiphoton microscopy. LSFMs produce well-registered serial sections that are suitable for three-dimensional reconstruction of tissue structures. Because of a lack of a commercial LSFM microscope, numerous versions of light sheet microscopes have been constructed by different investigators. This review describes development of the technology, reviews existing devices, provides details of one LSFM device, and shows examples of images and three-dimensional reconstructions of tissues that were produced by LSFM. (J Histochem Cytochem 59:129–138, 2011)

Keywords

OPFOS, TSLIM, light sheet microscopy, optical sectioning

Light sheet fluorescence microscopy (LSFM) uses a thin plane of light to optically section transparent tissues or whole organisms that have been labeled with a fluorophore. Table 1 shows that LSFM offers higher resolution (subcellular) and faster imaging speed compared with other nondestructive tomographic devices such as magnetic resonance imaging (MRI) and computerized tomography (CT). Compared with confocal and two-photon microscopy, LSFM is able to image thicker tissues (>1 cm) with reduced photobleaching and phototoxicity of a specimen because the specimen is exposed only to a thin light sheet. In addition, LSFM is a nondestructive method that produces well-registered optical sections that are suitable for three-dimensional reconstruction and can be processed by other histological methods (e.g., mechanical sectioning) after imaging. Furthermore, the cost to construct an LSFM device is much less compared to these other microscopes. This review describes development of the technology, reviews existing devices, provides details of one LSFM device, and shows examples of images and three-dimensional reconstructions of tissues that were produced by LSFM.

Development of Light Sheet Fluorescence Microscopy

The first published account of a very simple version of an LSFM (called ultramicroscopy) was described by Siedentopf and Zsigmondy (1903) in which sunlight was projected through a slit aperture to observe gold particles (Fig. 1). However, this article did not stimulate further development of LSFM. In 1993, Voie and colleagues developed a light sheet microscope system, called orthogonal-plane fluorescence optical sectioning (OPFOS), and introduced it into the current literature in a *Journal of Microscopy* paper (Voie et al. 1993). OPFOS was developed

Received for publication September 30, 2010; accepted November 14, 2010

Corresponding Author:
Peter A. Santi, Department of Otolaryngology, University of Minnesota, Room 121, Lions Research Building, 2001 Sixth St. SE, Minneapolis, MN 55455.
E-mail: psanti@umn.edu

by investigators in Francis Spelman's laboratory at the University of Washington who were attempting to quantitatively assess hair cell structure and other cochlear features to improve the cochlear implant. This is a difficult task because of the spiral anatomy of the cochlea. The cochlea is embedded in bone and contains three spirally directed, fluid-filled canals. Within the central canal (i.e., scala media) lie the hair cells of the organ of Corti that are located on the basilar membrane. Hair cells form a repeating array of cells that travel around a central core from the base to the apex of the cochlea. To produce a map, called a cytocochleogram, of hair cell damage along the length of the basilar membrane, it is necessary to visualize and assess all of the hair cells along the length of the basilar membrane. This map is used to relate hair cell morphology with functional deficits in hearing because frequencies are mapped from high to low from the cochlear base to the apex.

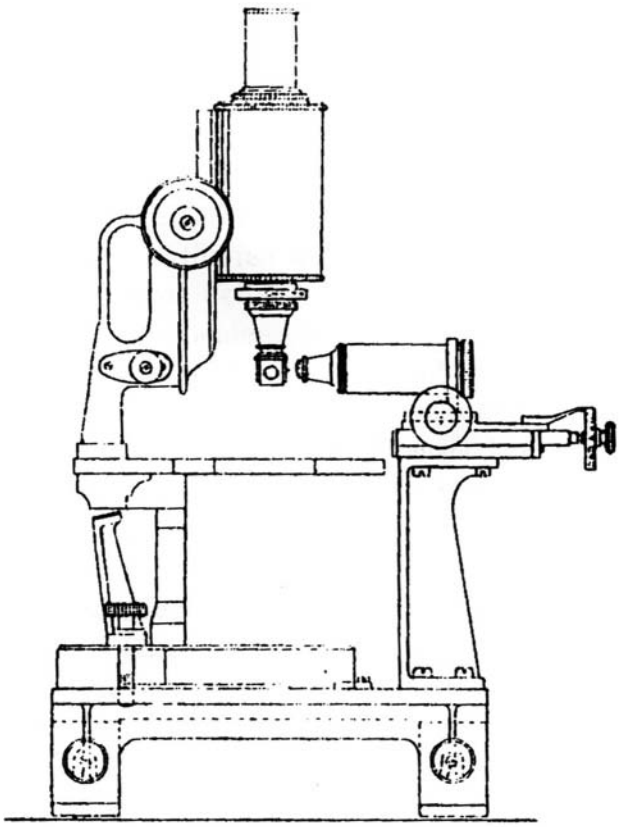

Figure 1. This is Figure 3 from Siedentopf and Zsigmondy's (1903) article and shows part of their light sheet microscope with an upright microscope containing a specimen holder that appears to be mounted to its objective lens and orthogonal illumination at 90° from what appears to be an illuminating objective. The slit aperture and collection of sunlight is shown in another figure (not shown). Magnifications were not provided.

Perry Santos (1986) developed a method to perform a three-dimensional reconstruction of the cochlea using mechanical sections; however, mechanical sections are not ideal for producing three-dimensional reconstructions because of compression and registration artifacts. Nadeem Haq (1988) described an imaging method in which the complete length of the organ of Corti could be observed in the whole cochlea by making the bone transparent after fixation and decalcification using a clearing solution (Spalteholtz 1914). Although the organ of Corti was stained and visualized, it was still difficult to assign accurate three-dimensional coordinates along the length of the basilar membrane. David Burns (who came up with the OPFOS name) noticed what appeared to be a sectioned pig embryo on the front cover of a book on photomacrography (White 1987), and within the book was a description of a microscope using side illumination called a Dynaphot. Photomacrography using a side illuminating light sheet (produced by a slit aperture) for examining surface features of structures was also previously described by several investigators (McLachlan 1964; Simon 1965). From the example of side illuminating photomacrography, Arne Voie with David Burns and Francis Spelman developed the OPFOS device and used it to optically section, for the first time, whole fluorophore-stained and cleared cochleas (Voie et al. 1993; Voie and Spelman 1995; Voie 1996, 2002). OPFOS featured all of the elements that are present in current LSFM devices—namely, laser, beam expander, cylindrical lens to generate the light sheet, specimen chamber, orthogonal illumination of the specimen, specimen movement for z-stack creation, and specimen clearing and staining for producing fluorescent optical sections.

In 1994, but unknown to Voie and colleagues, an oblique illuminating confocal microscope was being developed in Germany in Ernst Stelzer's laboratory to improve the axial resolution of confocal microscopy. It was called a confocal theta microscope (Lindek et al. 1994; Lindek and Stelzer 1994; Stelzer et al. 1995). Their 1995 article cited Voie's work on OPFOS, and theta confocal microscopy appeared to lay the foundation for their subsequent version of an LSFM device called selective or single-plane illumination microscopy (SPIM).

Although Voie and colleagues published several articles (Voie et al. 1993; Voie and Spelman 1995; Voie 1996, 2002) in widely read journals, it was not until the publication of the SPIM paper in 2004 in *Science* (Huisken et al. 2004) that development and use of LSFM were accelerated. This article highlighted the usefulness of LSFM for investigating embryonic development and included imaging of heartbeats and green fluorescent protein in ganalion cells in live medaka embryos (*Oryzias latipes*) and embryogenesis of a *Drosophila melanogaster* embryo over a 17-hr period. A number of other LSFMs have been developed since Voie's original description, and their features are compared in Table 2. The reader will notice, and it has been pointed out

Table 1. Microscope Comparisons

Name	Signal	Resolution	Fluorescent	Size	Imaging Time	Cost ($)	Photobleaching	Citation
Magnetic resonance imaging	Magnetic	mm	No, contrast agent	M	hr	Millions	NA	Lauterbur 1973
Computed tomography	Radioactive	<mm	No, contrast agent	cm	min	Millions	NA	Kalender 2006
Confocal	Laser	<micron	Yes	micron	msec	200,000	Yes	Minsky 1961
2-Photon	Laser	<micron	Yes	mm	msec	500,000	Less	Denk et al. 1990
Light sheet fluorescence microscopy	Laser	micron	Yes	>cm	msec	30,000	Least	Voie et al. 1993

The signal refers to the type of excitation. Resolution is approximate and refers to the average resolution provided by different instruments. Fluorescent refers to whether the instrument is capable of detecting fluorescent probes. Size refers to the size of the specimen that can be imaged. Time refers to the average time it takes to make a stack of the specimen that is within the size range of the imaging device. Cost is approximate, and photobleaching refers to how quickly the fluorescent probe fades. NA not applicable.

in other reviews of LSFM (Greger et al. 2007; Reynaud et al. 2008; Huisken and Stainier 2009), that each investigator has developed a somewhat different system and given it a different name and acronym. A group of these developers has been formed to agree on terminology (with LSFM being the general term) and to optimize development of LSFM (Reynaud and Tomancak 2010).

Referring to Table 2, Fuchs et al. (2002) described an OPFOS-like device, which they called a thin laser light sheet microscope (TLSM), to examine microorganisms in seawater. To image large specimens such as the brain and make the illumination more uniform across the width of the specimen, Dodt and colleagues (Dodt et al. 2007; Becker et al. 2008) added dual-sided illumination to LSFM and called their method "ultramicroscopy" after the original name given by Siedentopf and Zsigmondy (1903). However, this does not appear to be a good name since a PubMed search for *ultramicroscopy* yields 2254 citations, and almost all of the citations relate to electron microscopy. Dual-sided illumination also minimized shadow artifacts or stripes, which are dark lines across a large specimen that are produced when light encounters an opaque structure as it travels across the tissue plane. Becker et al. (2008) showed labeling of nerve fibers in E12.5 mouse embryo using whole-mount immunohistochemistry with a primary antibody that recognized neurofilaments. Huisken and Stainier (2007) reduced shadow artifacts by pivoting the cylindrical lens in a device called mSPIM. Leischner et al. (2010) addressed the problem in a different way by developing a stripe-removal algorithm. Another problem with early LSFM devices for imaging large specimens is caused by the geometry of the light sheet. A light sheet formed by a cylindrical lens has a Gaussian beam profile with a minimum thickness at its focal point called the beam waist. Beam thickness increases on both sides of the beam waist, and the distance where it remains relatively constant is called the confocal parameter. If the width of a specimen is larger than the confocal parameter, then it will appear to be in focus only along the distance of the confocal parameter. For example, for a light sheet with a thickness of 4 μm, the confocal parameter is only 68 μm. Buytaert and Dirckx (2007) resolved this problem by scanning the specimen across the beam waist and "stitching" single-image columns together to form a well-focused, composite image across the full width of a large specimen. They called their microscope a high-resolution OPFOS or HROPFOS. Instead of moving the specimen in the z-axis for optical sectioning, Holecamp et al. (2008) and Turaga and Holy (2008) attached the light sheet illuminator to the observing objective and called their device objective-coupled planar illumination (OCPI) microscopy. Dunsby (2008) developed an LSFM that uses a single, high numeric aperture (NA) objective to both illuminate a plane in a sample and to collect the fluorescence with an oblique light sheet and called their device oblique plane microscopy (OPM). The authors propose that OCPI and OPM can be fitted to existing microscopes for imaging small specimens. Keller and colleagues (Keller et al. 2008; Keller and Stelzer 2008; Keller et al. 2010) produced another type of LSFM called a digital scanned laser light sheet fluorescence microscope (DSLM). This device produces a line-like laser beam (using an f-theta lens) that is scanned across a small specimen, and the image is collected in the orthogonal plane. For in vivo development of zebrafish embryos over a 24-hr period, Keller and colleagues (2008) tracked nuclei that were labeled at the one-cell stage by mRNA injection of H2B-eGFP, which localizes chromatin. Mertz and Kim (2010) described a HiLo LSFM that uses structured illumination to reject out-of-focus background signal to improve imaging. In 2009, we developed an LSFM called thin-sheet laser imaging microscopy (TSLIM) that incorporated many of the previous design features for imaging large specimens such as the inner ear, brain, and zebrafish (Santi et al. 2009). TSLIM will be described in more detail as an example of an LSFM that can be constructed by an investigator.

Table 2. LSFM Types and Features

Name/Acronym	Date	Light Source	Light Sheet	Detection Angle, °	Illumination	Specimen Size	Citation
Ultramicroscopy	1903	Sunlight	Slit aperture	90	Single	Gold beads	Siedentoph and Zsigmondy 1903
OPFOS	1993	532-nm laser	Cylindrical lens	90	Single	Cochlea >1 cm	Voie et al. 1993; Voie and Spelman 1995; Voie 2002
Theta confocal	1995	450-, 550-nm laser	Pinhole, not light sheet	102	Single	<1 cm	Stelzer et al. 1995
TSLM	2002	540-nm laser	Cylindrical lens	90	Single	>1 cm	Fuchs et al. 2002
SPIM	2004	488-nm laser	Cylindrical lens	90	Single	<1 cm	Huisken et al. 2004
mSPIM	2007	488-nm laser	Pivoting cylindrical lens	90	Dual	<1 cm	Huisken and Stainier 2007
HROPFOS	2007	532-nm laser	Cylindrical lens	90	Single	>1 cm	Buytaert and Dirckx 2007
Ultramicroscopy	2007	488-nm laser	Cylindrical lens	90	Dual	>1 cm	Dodt et al. 2007
OPM	2008	532-nm laser	Cylindrical lens	60	Single	<1 cm	Dunsby 2008
OCPI	2008	488-nm laser	Cylindrical or gradient index lens	90	Single	<1 cm	Holekamp et al. 2008
DSLIM	2008	400- to 650-nm laser	f-theta lens	90	Dual	<1 cm	Keller et al. 2008; Keller and Stelzer 2008; Keller et al. 2010
TSLIM	2009	532-, 488-nm laser	Cylindrical lens	90	Dual	>1 cm	Santi et al. 2009
HiLo	2010	491-nm laser	Scanned line	0	Single	>1 cm	Mertz and Kim 2010

Only the first or most relevant citation is given. The detection angle is the angle between the light sheet and detecting objective. Specimen chamber size is an approximate maximum because many investigators do not accurately state this, but with immersion objectives, specimen size usually is less than 1 cm. OPFOS, orthogonal-plane fluorescence optical sectioning; TLSM, thin-light sheet microscopy; SPIM, selective or single-plane illumination microscopy; mSPIM, multidirectional selective plane illumination microscopy; HROPFOS, high-resolution orthogonal-plane fluorescence optical sectioning; OPM, oblique plane microscopy; OCPI, objective-coupled planar illumination; DSLIM, digital scanned laser light sheet microscope; TSLIM, thin-sheet laser illuminating microscopy.

Instrumentation

Thin-Sheet Laser Imaging Microscope (TSLIM)

Like most LSFMs, TSLIM consists of several fundamental parts: illuminator, specimen chamber, detection apparatus, and computer-controlled motorized micropositioners for specimen movement, all of which are positioned on an antivibration table. Figure 2 is a diagram showing most of these parts. The illuminator consists of a laser, a beam expander to fill the cylindrical lens, a cylindrical lens to produce a light sheet, and an illuminating objective to reduce light aberrations produced by the cylindrical lens. The focal point (or beam waist) of the light sheet is placed within the specimen chamber at the focal plane of the detecting objective, which, in the case of TSLIM, is determined by the objective lens of an Olympus MVX macroscope. Two different-colored lasers (532 nm, 488 nm) are used to visualize a wide range of biologically useful fluorophores, such as rhodamine; fluorescein; green, yellow, and red fluorescent protein; and some of the Alexa dyes, to name a few. TSLIM contains a second illuminator that is positioned opposite the first illuminator (at 180°) and projects an opposing light sheet into the specimen chamber (not shown in Figure 2). Dual-sided illumination reduces shadow artifacts and provides for more intense and even illumination of a large specimen. A disadvantage of dual-sided light sheets is that it is difficult to perfectly align both light sheets in three-dimensional space, with the result that the optical section does not appear as well focused as with single-sided illumination. A barrier filter is placed in the optical path of the detecting objective and is used to exclude the laser light signal but allow passage of fluorescence emitted by the light sheet plane within the tissue. An advantage of using a microscope such as the Olympus MVX, instead of an objective and tube lens, is that the microscope contains a filter wheel and zoom magnification

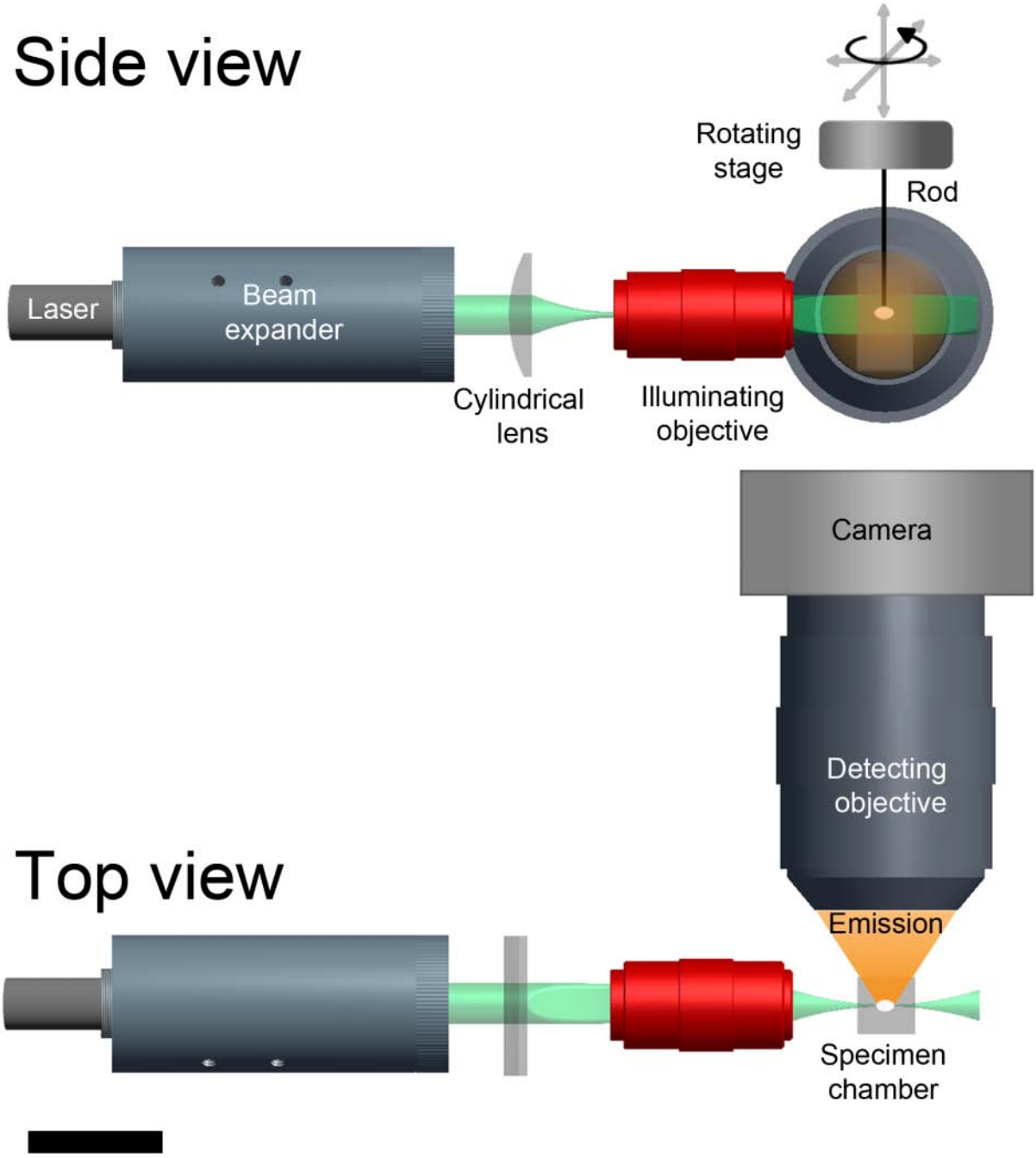

Figure 2. A diagram showing a side and top view of the basic components of a light sheet fluorescence microscope (LSFM). The light sheet is formed by a laser (solid state or gas) and is collimated and expanded with a beam expander. A cylindrical lens forms the light sheet (green beam), and it is projected through an illuminating objective. The focal point or the thinnest portion of the light sheet is positioned usually within the middle of the specimen chamber. The specimen chamber is made of optically clear glass walls and has an open top for specimen insertion. The chamber is filled with either a warmed physiological solution for live-cell imaging or clearing fluid for fixed and cleared tissue. The specimen (white ellipsoid) is attached to a rod and is intersected by the light sheet and a fluorescent plane (i.e., optical section) within the tissue (labeled emission [orange cone]), which is collected by a microscope that is usually mounted in a horizontal position. The specimen rod is attached to rotating and translating stages (not shown) for micropositioning. For a small specimen or a relatively thick light sheet, the fluorescent plane within the tissue is collected by a digital camera as a real-time two-dimensional optical section. However, for specimens larger than the distance of the confocal parameter of the light sheet, the specimen is scanned in the x-axis to produce a well-focused composite image across the width of the specimen. By moving the specimen in the z-axis and collecting another image, a stack of well-aligned, serial optical sections (i.e., a z-stack) through the tissue is obtained. Bar = 5 cm.

adjustment for optimized specimen viewing and recording by a digital camera. The placement of the objectives in the air rather than immersed in the specimen chamber (like SPIM, mSPIM, and DSLM) allows more flexibility. Different lenses and different-size specimen chambers can be rapidly changed to accommodate different-size specimens. Immersed objectives provide higher magnification and better resolution because of their higher NA but at the cost of a reduced focal depth. Immersed lenses are fixed within the specimen chamber and cannot be moved to accommodate different-size specimens. In addition, the long-term effect on the mounting material of the objective lenses that are immersed in a strong solvent such as methyl salicylate/benzol benzoate is not known.

TSLIM specimen chambers consist of different-size fluorometer cells that have optically clear walls, fused wall joints, and an open top to insert a specimen. A cleared specimen is attached to a black Delrin (Dupont, Wilmington, DE) rod by gluing (using 1 min clear epoxy) or by a spring that is attached to the specimen and the rod. Fixed and cleared specimens are inserted into the specimen chamber containing a clearing solution for imaging. Because clearing solutions are solvents, they react with most plastics and glues, which present specimen-mounting problems. For live specimens, the rod is attached to an agarose cylinder containing a specimen that is immersed in warmed physiological solution rather than in a clearing solution. In either case, the upper portion of the specimen rod is attached to a motorized, rotating stage for positioning the specimen and for multiview imaging. Multiview imaging is desirable if there are objects in the specimen that block the light path (e.g., pigmented eyes in zebrafish embryos); the specimen can be rotated, and multiple stacks at different angles are collected and later merged together to provide for complete imaging of the specimen. The rotating stage is attached to motorized x,y,z-axes stages (not shown in Fig. 2) for moving the specimen through the light sheet. Movement in the x-axis produces a well-focused specimen across its full width. Movement in the y-axis positions the specimen within the focal plane of the detecting objective, and movement in the z-axis produces a stack of serial, optical sections through the specimen. Specimen movement and collection of images are performed by a user-written LabVIEW program and Newport servomotor control systems (Santi et al. 2009). Two digital cameras are used with TSLIM: a Retiga 2000R CCD camera (QImaging, Surrey, British Columbia, Canada) and a DALSA HS-40 (DALSA, Waterloo, Ontario, Canada) line scan camera (Schacht et al. 2010).

A TSLIM imaging session consists of loading the specimen, positioning and focusing the specimen within the field of view, repositioning the specimen at the beginning of its thickness, and collecting a stack of images through the full thickness and width of the specimen. A magnification is usually selected to include the whole size of the organ or organism to fit within a single image, which facilitates three-dimensional reconstruction of structures and morphometric computations. However, higher magnification stacks of a portion of a specimen are also obtained. Photobleaching and phototoxicity are not a significant problem for repeated imaging and collection of multiple stacks from a single specimen as compared to wide-field fluorescent, confocal, and multiphoton microscopy. Schacht et al. (2010) showed only a 13% reduction in fluorescence in an optical section that was repeatedly imaged 50 times over 475 sec. Typically, only a few stacks are obtained from a single specimen, and we have examined specimens that were stored in clearing solution in the dark for several months that did not show a significant reduction in staining intensity.

Specimen Processing

Because LSFM is an optical method, biological specimens need to be transparent and fluorescent for imaging. Pigments and other optically opaque substances (such as calcium) must be removed (by EDTA chelation) or be made transparent by preventing pigment formation (with 1-phenyl 2-thiourea [PTU]) for zebrafish embryos (Karlsson et al. 2001) or bleaching of pigment with hydrogen peroxide (Korytowski and Sarna 1990) and, most commonly for thick tissues, by chemically clearing with methyl salicylate/benzyl benzoate (Spalteholz 1914) or benzyl alcohol/benzyl benzoate (Klymkowsky and Hanken 1991) for imaging. Although all LSFM devices can image both live and fixed and cleared tissues, some devices (e.g., SPIM, mSPIM, and DSLIM) are optimized for imaging small, live specimens such as developing embryos.

Because LSFM is a fluorescent method, fluorophores or some type of fluorescent molecule must be incorporated within the tissue. Autofluorescence after formalin fixation (Leischner et al. 2010), shown in Figure 3A, and even brighter autofluorescence after glutaraldehyde fixation have been used to image tissue by LSFM. However, the addition of fluorescent molecules to a tissue increases the staining intensity, which reduces stack collection times. Voie and colleagues (1993) stained their cochlear specimens en bloc by adding rhodamine B isothiocynate to the clearing solution. This staining procedure has also been successfully used for TSLIM imaging using a variety of different tissues, including brain, zebrafish heads, and mouse cochleas (Fig. 3). In an unstained rat brain (Fig. 3A), neurons appear as dark structures against a lighter background. In a rhodamine-stained zebrafish head, bony structures of the skull and inner ear appear bright and well stained, as does the brain, with the nerve fiber tract bundles appearing as lightly stained. In the rhodamine-stained mouse cochlea, bony tissue and all of the cells and connective tissues within the scala media are bright and well stained, including the hair cells of the organ of Corti, tectorial membrane, stria

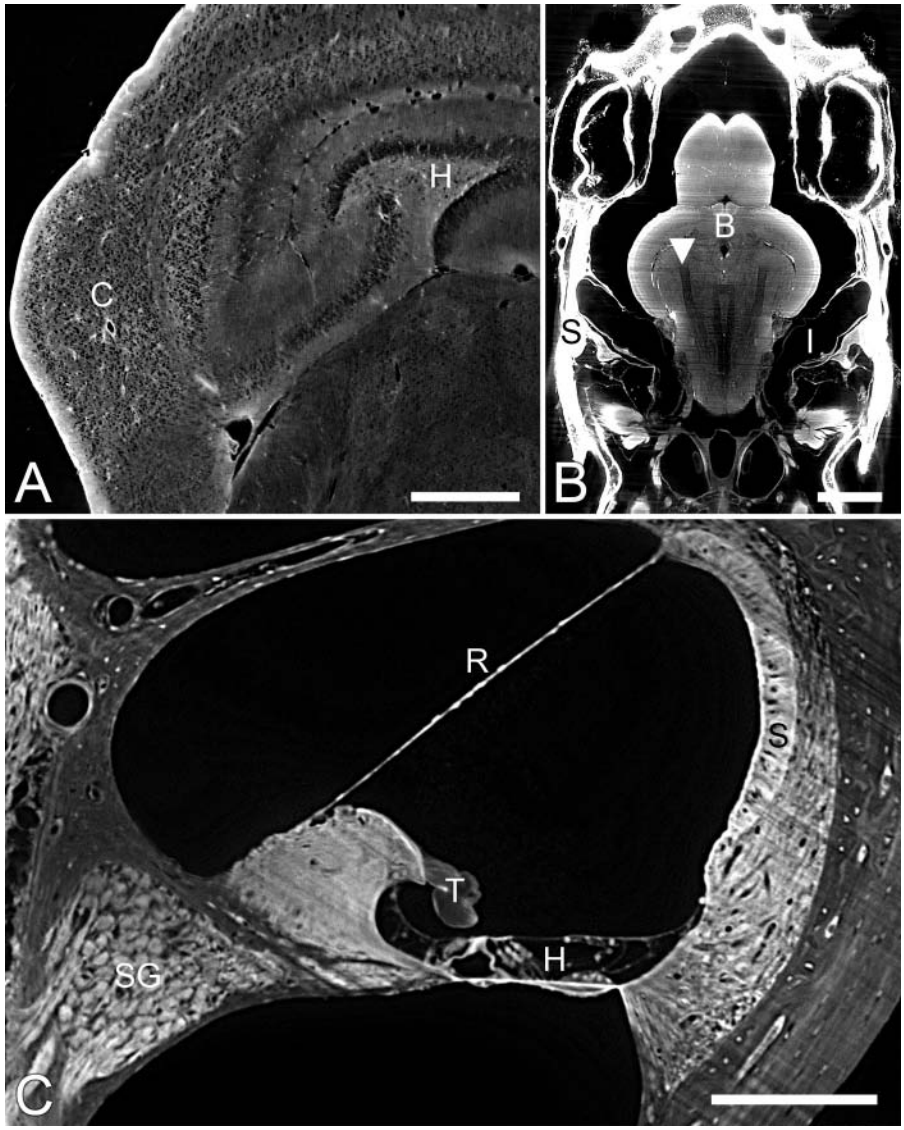

Figure 3. Thin-sheet laser imaging microscopy optical sections from a rat brain, zebrafish head, and mouse cochlea. (A) An optical section from a z-stack from a paraformaldehyde-fixed, unstained rat pup brain (5 weeks old). Neurons are seen as dark structures in the cortex (C) and hippocampus (H) against a lighter background. The image was taken with the line scan camera and adjusted for brightness, contrast, unsharp masking, contrast-limited adaptive histogram equalization, and fast Fourier transform for line shadow reduction. Bar = 500 µm. (B) Rhodamine-stained zebrafish head showing brightly stained bones of the skull (S) and inner ear (I) and lighter staining of the brain (B) with nerve fiber bundles (arrowhead) shown as lightly stained structures. The image was taken with the Retiga CCD camera and adjusted for brightness, contrast, unsharp masking, and fast Fourier transform for line shadow reduction. Bar = 500 µm. (C) Scala media cross section from a mouse cochlea stained with rhodamine showing hair cells (H) of the organ of Corti, tectorial membrane (T), stria vascularis (S), spiral ganglion neurons (SG), and Reissner's membrane (R). The image was taken with the line scan camera and adjusted for brightness, contrast, and unsharp masking. Bar = 100 µm.

vascularis, spiral ganglion neurons, and the two–cell layer Reissner's membrane. In addition, because the cochlea contains fluid-filled chambers and thin layers of cells, inner ear structures can be specifically labeled using indirect immunohistochemistry. Figure 4 shows labeling of the outer hair cells with an antibody to prestin, which is an anion transporter and motor protein that is contained in the lateral wall of the outer hair cells. For other tissues that are more compact such as the brain, it is possible to visualize yellow fluorescent protein (YFP) but not green fluorescent protein (GFP) or red fluorescent protein (RFP) in transgenically expressed fluorescent neurons (not shown). It seems that

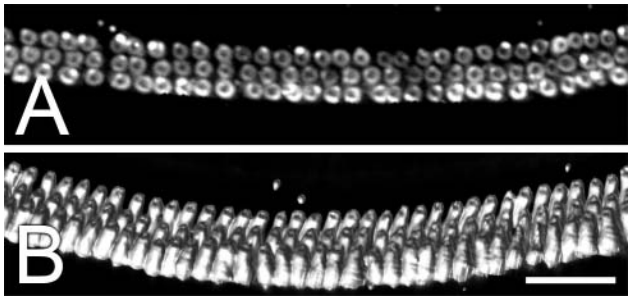

Figure 4. Thin-sheet laser imaging microscopy image of the mouse organ of Corti showing outer hair cells labeled with a prestin antibody. (A) The secondary antibody was coupled to the Alexa Fluor 532 fluorophore and showed the presence of the primary antiprestin antibodies within the lateral wall of the outer hair cells where they serve as motor proteins for the outer but not the inner hair cells. (B) An Amira three-dimensional isosurface reconstruction of these prestin-labeled outer hair cells showing the distribution of this protein in the middle but not apical and basal portion of the outer hair cells. The image was taken with the line scan camera and adjusted for brightness and contrast, as well as masked to show only the organ of Corti, and the background was subtracted to remove haze. Bar = 500 µm.

dehydration leaches or quenches GFP and RFP and prevents their detection in tissues cleared for TSLIM imaging. Specimen processing remains an important consideration for LSFM imaging for fixed, dehydrated, and cleared tissues.

Image Processing

LSFM is capable of producing a large number of optical sections. Strategies to effectively classify, sort, and retrieve metadata from images are being developed in the Open Microscopy Environment, for example (Swedlow 2010), but this remains a challenging problem. Two-dimensional images produced by an LSFM are generated either from a real-time two-dimensional section or from a scanned composite image of single or averaged lines of image column data. The two-dimensional images often undergo multiple adjustments in exposure, contrast, deconvolution, fast Fourier transform, unsharp masking, and other processing steps to yield a "well-corrected" image. Two-dimensional images are often combined or registered with other two-dimensional images from multiviews of the same specimen to reveal structures that were occluded by opaque structures. However, the primary goal for collecting a z-stack of two-dimensional images is to produce three-dimensional reconstruction of specific structures by segmentation or outlining of structures in all of the two-dimensional images in a stack. Segmentation is usually a time-consuming, manual procedure, but methods are being developed in combination with specific labeling to automate the segmentation process. Three-dimensional rendered structures are often used not only to visualize their three-dimensional anatomy but also to estimate their morphometric parameters such as length and volume. Rendering and particularly smoothing methods used to produce three-dimensional renderings of structures need to be considered to determine how these methods affect the accuracy of the morphometric estimates.

Conclusions and Future Directions

LSFMs are being developed and improved in a number of laboratories at a rapid pace. This is probably because of LSFMs' ability to rapidly produce high-quality, well-registered optical sections of small and large, live and fixed tissues and whole organisms, with minimal photobleaching and phototoxicity of the specimen. LSFM occupies a niche between the confocal/multiphoton microscopes and the magnetic-based, low-resolution microscopes. LSFM devices are being enhanced for higher resolution and faster imaging times. Current developers are applying structured illumination, stimulated emission depletion, and two-photon and other instrument modifications to LSFM to improve its resolution. Specimen processing is also being addressed using novel ways to preserve fluorophores such as green and red fluorescent proteins that are not retained or expressed in tissues that have been fixed, dehydrated, and cleared. Whole-tissue immunohistochemical antibody methods and fluorophore-labeled molecules are also being used in LSFM to specifically label tissues structures and to allow for automatic segmentation. Last, a commercial instrument will greatly improve the capabilities and use of this microscopic method for three-dimensional reconstruction of tissue structures.

Acknowledgments

I thank the following individuals for their excellent assistance in the development of TSLIM: two engineering students (Matthias Hillenbrand and Peter Schacht) from the Technical University of Ilmenau who made TSLIM a functional and reliable instrument; Shane Johnson for his excellent work on tissue processing, TSLIM imaging, drawing of Figure 2, and image processing; Heather Schmitz for her excellent segmentation of inner ear structures; Dr. Marilyn Carroll and Justin Anker (University of Minnesota) for the rat pub brain tissue; and Richard White (Children's Hospital Boston) for the Casper zebrafish tissue. The care and use of the animals in this study have been approved by the University of Minnesota's Institutional Care and Use Committee and have been approved by the National Institutes of Health, which has funded this research.

Declaration of Conflicting Interests

The author(s) declared no potential conflicts of interest with respect to the authorship and/or publication of this article.

Funding

The author(s) disclosed receipt of the following financial support for the research and/or authorship of this article: This work was supported by the Capita Foundation and grants from the National Institute on Deafness and Other Communication Disorders (RO1DC007588 and RO1DC007588-03S1).

References

Becker K, Jährling N, Kramer ER, Schnorrer F, Dodt HU. 2008. Ultramicroscopy: 3D reconstruction of large microscopical specimens. J Biophotonics. 1:36-42.

Buytaert JA, Dirckx JJ. 2007. Design and quantitative resolution measurements of an optical virtual sectioning three-dimensional imaging technique for biomedical specimens, featuring two-micrometer slicing resolution. J Biomed Opt. 12:014039.

Denk W, Strickler J, Webb W. 1990. Two-photon laser scanning fluorescence microscopy. Science. 248:73-76.

Dodt HU, Leischner U, Schierloh A, Jährling N, Mauch CP, Deininger K, Deussing JM, Eder M, Zieglgsnsberger W, Becker K. 2007. Ultramicroscopy: three-dimensional visualization of neuronal networks in the whole mouse brain. Nat Methods. 4:331-336.

Dunsby C. 2008. Optically sectioned imaging by oblique plane microscopy. Opt Express. 16:20306-20316.

Fuchs E, Jaffe J, Long R, Azam F. 2002. Thin laser light sheet microscope for microbial oceanography. Opt Express. 10: 145-154.

Greger K, Swoger J, Stelzer EHK. 2007. Basic building units and properties of a fluorescence single plane illumination microscope. Rev Sci Inst. 78:023705-023707.

Haq N. 1988. Application and evaluation of an imaging technique for 3-deminsional cochlear reconstruction [master's thesis]. [Seattle (WA)]: University of Washington.

Holekamp TF, Turaga D, Holy TE. 2008. Fast three-dimensional fluorescence imaging of activity in neural populations by objective-coupled planar illumination microscopy. Neuron. 57:661-672.

Huisken J, Stainier DY. 2007. Even fluorescence excitation by multidirectional selective plane illumination microscopy (mSPIM). Opt Lett. 32:2608-2610.

Huisken J, Stainier DY. 2009. Selective plane illumination microscopy techniques in developmental biology. Development. 136:1963-1975.

Huisken J, Swoger J, Del Bene F, Wittbrodt J, Stelzer EH. 2004. Optical sectioning deep inside live embryos by selective plane illumination microscopy. Science. 305:1007-1009.

Kalender WA. 2006. X-ray computed tomography. Phys Med Biol. 51:29-43.

Karlsson J, von Hofsten J, Olsson PE. 2001. Generating transparent zebrafish: a refined method to improve detection of gene expression during embryonic development. Mar Biotechnol. 3:522-527.

Keller PJ, Schmidt AD, Santella A, Khairy K, Bao Z, Wittbrodt J, Stelzer EH. 2010. Fast, high-contrast imaging of animal development with scanned light sheet-based structured-illumination microscopy. Nat Methods. 7:637-642.

Keller PJ, Schmidt AD, Wittbrodt J, Stelzer EH. 2008. Reconstruction of zebrafish early embryonic development by scanned light sheet microscopy. Science. 322:1065-1069.

Keller PJ, Stelzer EH. 2008. Quantitative in vivo imaging of entire embryos with digital scanned laser light sheet fluorescence microscopy. Curr Opin Neurobiol. 18:624-632.

Klymkowsky MW, Hanken J. 1991. Whole mount staining of Xenopus and other vertebrates. Methods Cell Biol. 36: 419-441.

Korytowski W, Sarna T. 1990. Bleaching of melanin pigments: role of copper ions and hydrogen peroxide in autooxidation and photooxidation of synthetic dopa-melanin. J Biol Chem. 265:12410-12416.

Lauterbur PC. 1973. Image formation by induced local interactions: examples of employing nuclear magnetic resonance. Nature. 242:190-191.

Leischner U, Schierloh A, Zieglgansberger W, Dodt HU. 2010. Formalin-induced fluorescence reveals cell shape and morphology in biological tissue samples. PLoS One. 5:1-8.

Lindek S, Pick R, Stelzer EHK. 1994. Confocal theta microscope with three objectives lenses. Rev Sci Instr. 65:3367-3372.

Lindek S, Stelzer EHK. 1994. Confocal theta microscopy and 4Pi-confocal theta icroscopy. SPIE Proc. 2184:188-194.

McLachlan D. 1964. Extreme focal depth in microscopy. Appl Opt. 3:1009-1014.

Mertz J, Kim J. 2010. Scanning light-sheet microscopy in the whole mouse brain with HiLo background rejection. J Biomed Opt. 15:01627-01634.

Minsky M. 1961. Microscopy apparatus. United States patent US 301467. December 1961.

Reynaud EG, Krzic U, Greger K, Stelzer EH. 2008. Light sheet-based fluorescence microscopy: more dimensions, more photons, and less photodamage. HFSP J. 2:266-275.

Reynaud EG, Tomancak P. 2010. Meeting report: First light sheet based fluorescence microscopy workshop. Biotechnol J. 5:798-804.

Santi PA, Johnson SB, Hillenbrand M, GrandPre PZ, Glass TJ, Leger JR. 2009. Thin-sheet laser imaging microscopy for optical sectioning of thick tissues. Biotechniques. 46:287-294.

Santos MPA. 1986. A computer assisted morphometric method for 3-dimensional morphological reconstruction of the cochlea [master's thesis]. [Seattle (WA)]: University of Washington.

Schacht P, Johnson SB, Santi PA. 2010. Implementation of a continuous scanning procedure and a line scan camera for thin-sheet laser imaging microscopy. Biomed Opt Express. 1:598-609.

Siedentopf H, Zsigmondy R. 1903. Über Sichtbarmachung und Groessenbestimmung ultramikroskopischer Teilchen, mit besonderer Anwendung auf Goldrubinglaesern. Annalen der Physik. 10:1-39.

Simon W. 1965. Photomicrography of deep fields. Rev Sci Inst. 36:1644-1655.

Spalteholz W. 1914. Über das Durchsichtigmachen von menschlichen und tierischen Päparaten. Leipzig, Germany: S. Hierzel.

Stelzer EHK, Lindek S, Albrecht S, Pick R, Ritter G, Salmon NJ, Stricker R. 1995. A new tool for the observation of embryos and other large specimens: confocal theta fluorescence microscopy. J Microsc. 178:1-10.

Swedlow J. 2010. Open Microscopy Environment (OME). http://www.openmicroscopy.org/site

Turaga D, Holy TE. 2008. Miniaturization and defocus correction for objective-coupled planar illumination microscopy. Opt Lett. 33:2302-2304.

Voie AH. 1996. Three-dimensional reconstruction and quantitative analysis of the mammalian cochlea [dissertation]. [Seattle (WA)]: University of Washington.

Voie AH. 2002. Imaging the intact guinea pig tympanic bulla by orthogonal-plane fluorescence optical sectioning microscopy. Hear Res. 171:119-128.

Voie AH, Burns DH, Spelman FA. 1993. Orthogonal-plane fluorescence optical sectioning: three dimensional imaging of macroscopic biological specimens. J Microsc. 170:229-236.

Voie AH, Spelman FA. 1995. Three-dimensional reconstruction of the cochlea from two-dimensional images of optical sections. Comput Med Imaging Graph. 19:377-384.

White W. 1987. Photomacrography: an introduction. Boston: Focal Press.